3D Reconstruction of Patient Specific Bone Models from 2D Radiographs for Image Guided Orthopedic Surgery

P. Gamage*, S. Q. Xie and P. Delmas
Department of Mechanical Engineering
The University of Auckland
Auckland, New Zealand
e-mail: *ppuh001@aucklanduni.ac.nz

P. Xu
School of Engineering & Advanced Technology
Massey University
Auckland, New Zealand

Abstract— **Three dimensional (3D) visualization of anatomy plays an important role in image guided orthopedic surgery and ultimately motivates minimally invasive procedures. However, direct 3D imaging modalities such as Computed Tomography (CT) are restricted to a minority of complex orthopedic procedures. Thus the diagnostics and planning of many interventions still rely on two dimensional (2D) radiographic images, where the surgeon has to mentally visualize the anatomy of interest. The purpose of this paper is to apply and validate a bi-planar 3D reconstruction methodology driven by prominent bony anatomy edges and contours identified on orthogonal radiographs. The results obtained through the proposed methodology are benchmarked against 3D CT scan data to assess the accuracy of reconstruction. The human femur has been used as the anatomy of interest throughout the paper. The novelty of this methodology is that it not only involves the outer contours of the bony anatomy in the reconstruction but also several key interior edges identifiable on radiographic images. Hence, this framework is not simply limited to long bones, but is generally applicable to a multitude of other bony anatomies as illustrated in the results section.**

Keywords-3D Bone Reconstruction; Patient-Specific Bone Customization

I. INTRODUCTION

Three dimensional knowledge of the bony anatomy is vital to several orthopedic Image Guided Surgical (IGS) procedures. For instance, the custom design of implant components for arthroplasties based on patient-specific anatomical models has been proposed to overcome existing shortcomings of current generic designs [1, 2]. Osteotomy surgical planning is also aided through pre-operative 3D patient-specific anatomical models [3]. Furthermore, personalized finite element modeling has been performed by [4], through the use of 3D patient-specific anatomical models.

The related work in 3D reconstruction of bony anatomy based upon information gathered through 2D imaging modalities (x-ray, fluoroscopy or ultrasound) can be divided into two subgroups given the different inputs required. The first group contains methods based purely on the 2D images [5], while the second group contains methods based on a-priori knowledge of the considered anatomical structure as well as 2D images [3, 4, 6-9]. A majority of work has utilized a-priori knowledge to provide information not available through 2D modalities. These studies have employed three main types of a-priori knowledge (template models): statistical models, free form deformation (FFD) models and morphological measurements (coupled with a generic model).

Statistical model based reconstruction methodologies establishes the legal topology parameter variations of the anatomy under study and attempts to identify a specific subset of those parameters that match the patient under study [6-8]. Due to the high manual input required during the landmark identification stage, typically only specific regions of the bone are statistically modeled (e.g. proximal femur [6] or distal femur [7]). Moreover, large databases of anatomical models are required to learn the necessary variability in the statistical model. Work conducted by [3, 4] utilizes a generic surface model of the anatomy of interest and performs deformations based on the FFD control lattice movements. The FFD method is limited by the fact that it does not consider the topology of the object under deformation. The FFD transformations will apply to all nearby regions tending to unrealistically distort the object, unless the bounding box subdivides the mesh into individual parts. Morphological measurements based customization performs scaling on a generic model based on key measurements obtained through radiographs (e.g. condyle width [9]). The limitation here is that it fails to take into consideration the deformation variations that fall outside these key measurements used.

While existing methods discussed above are to a certain extent effective, they have a number of limitations with regards to accuracy of reconstruction, adaptability to other orthopedic cases and the level of manual intervention required. The work presented in this paper is motivated by these limitations. The remainder of the paper will document the proposed reconstruction framework and confer the results obtained through the testing performed.

II. MATERIALS AND METHODS

The proposed framework to achieve 3D reconstruction is outlined in Fig. 1. The 2D x-ray images are initially processed to extract the edge points that potentially form the femur boundary. A novel non-rigid registration is then performed between the edges identified in the x-ray image and the projected contour points of the generic model. The registration has been developed to be robust to occlusions,

978-0-7695-3866-2/09 $26.00 © 2009 IEEE
DOI 10.1109/DICTA.2009.42

outliers, noise and deformations which are inherent problems seen in edges extracted from radiographic images. The identified point correspondences will next be interpolated to create a 2D planar translational field in both the anterior and lateral viewpoints. This translational field will identify the deformations required by the 3D anatomical model in the equivalent viewpoint. Finally a full 3D translational field will be created through a thin plate spline based interpolation and the 3D generic anatomical data deformed accordingly.

The proposed shape reconstruction framework utilizes a generic 3D surface model to provide the necessary cross-sectional topology constraints. The use of generic surface models will ensure quick adaptability of the proposed framework to other orthopedic cases. This is in contrast to having statistical models of the anatomy, which would require building and processing a large dataset of the anatomy of interest. Furthermore, the authors have developed a non rigid registration algorithm to provide the necessary deformation information as opposed to a FFD based techniques to provide greater control over localized shape deformation.

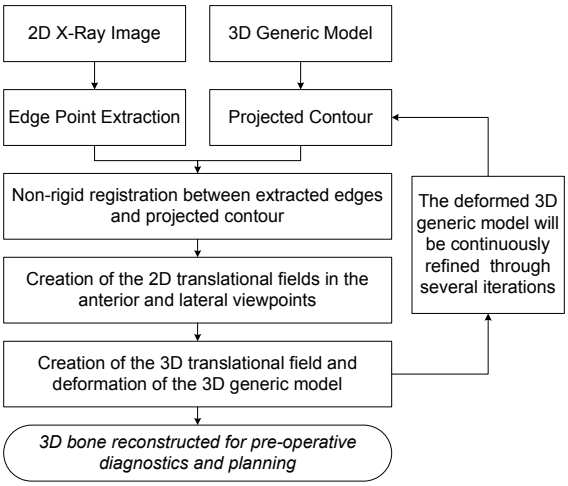

Figure 1. The main process steps of the proposed reconstruction framework.

A. *Anatomical Generic Model Preparation*

The numerous anatomical generic surface models utilized for our testing were all segmented and extracted from CT scan data. The generic models required certain automated pre-processing to identify the surface edge points that would be clearly identifiable on radiographic images. The outer contours in the frontal and lateral directions were identified through projection ray-tracing. The interior contours were classified utilizing the saddle points on the surface curvature. As an example, the femoral generic model is shown in Fig. 2 along with the outer and inner contours. Accurate identification of as many of these edges as possible on radiographic images is vital as the customization process is driven by them. This point is further discussed in the proceeding edge extraction section.

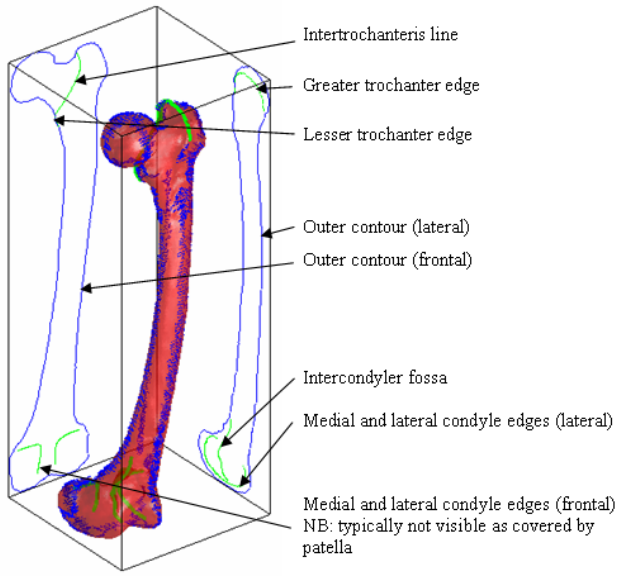

Figure 2. Example of the clearly identifiable edges on femur radiographic images. The blue lines form the outer contour while the green lines form the interior edges in the bi-planar radiographic images.

B. *Edge Extraction*

The main objective of the proposed edge extraction technique is to identify objects boundaries with sufficient continuity to be successfully employed in the proceeding shape based point correspondence estimation. Many of the classic first (Roberts, Prewitt, Sobel) and second (LOG) derivative based edge segmentation methodologies extract isolated edge pixels and do not provide continuous edge contours. The proposed edge extraction technique attempts to link sets of potential edge pixels to create continuous boundaries. It employs two tactics to achieve this: thresholding with hysteresis and edge relaxation.

Firstly, adaptive (local) hysteresis based thresholding is performed on the gradient image where the two threshold values are set to be the 50th and 75th percentile of gradient magnitude values in the local window. These threshold values were empirically chosen after multiple tests were conducted on x-ray images. Adaptive thresholding adjusts the threshold level according to the intensity statistics of a local region. This technique is employed typically with x-ray/fluoroscopic images to counter the illumination gradients present on the radiographs.

Secondly, edge relaxation is performed through a region growing exercise. This region growing is conducted on the intermediate pixels (pixels that fall between the 50th and 75th percentile of gradient magnitude values) to ensure sufficient continuity of the edge contour. Edge relaxation involves the recursive re-labeling of intermediate pixels with one or more neighboring edge pixels, utilizing an eight neighboring connectivity scheme. In-order to be reclassified as a foreground edge pixel, the difference of the magnitude and orientation of the intervening pixel with the surrounding edge pixels will be checked and has to be within a user specified tolerance level. Following the edge relaxation a

small component elimination morphological operation is performed to remove all connected pixel components with too few pixels. This is a noise elimination step that will remove any incorrectly identified edge contour pixels.

C. Shape Customization

The non-rigid registration between the 2D projective contours of the 3D generic model and the extracted edges of the patient-specific x-ray images is performed as the first step of the customization process. The registration is performed through a point correspondence estimation between the two point sets. Correspondence algorithms generally consist of two parts, firstly a similarity measure which provides a measure of "correspondence" between two pairs of points or features in different images, and secondly, a cost function that analyses the values produced by the similarity measure to identify a series of one-to-one matches between the points on those images. The similarity measure utilized in this case needs to be robust to several factors that are inherent problems seen in edges extracted in x-ray images. These factors include: disturbances (noise), deformations (shape and affine), outliers and occlusions.

A novel similarity measure was developed, in order to cater for the variety of factors discussed above and is separated into several components that utilize four key features: topology information, edge orientation, curvature and continuity (distance). The overall similarity measure will be a weighted combination of the individual similarities. It has been noted empirically that the use of multiple features reduces the discriminatory power of the individual features and leads to improved results.

Topology (or shape) based point matching is critical as it drives the correspondence between salient features of the objects. The shape descriptor introduced in this paper is one based on shape histograms which describe the distribution of a series of points with respect to a given point on a shape. Termed Shape Context, this descriptor was introduced in [10, 11]. The shape context based cost function (C_{shape}) to match a point P_m on the model contour to a point P_t on the target contour can be expressed as (1), where $h_m(n)$ and $h_t(n)$ denote the N-bin histogram (normalized) at P_m and P_t. Due to the χ^2 test used as the matching cost between the two shapes the C_{shape} similarity measure is intrinsically bounded in [0,1].

$$C_{shape}(p_m, p_t) = \frac{1}{2}\sum_{n=1}^{N}\frac{\left(h_m(n) - h_t(n)\right)^2}{h_m(n) + h_t(n)} \tag{1}$$

The primary benefit of utilizing this measure is that it is invariant to translation, rotation, scale and shape deformation of the two shapes under consideration. Due to these benefits the wide spread use of the shape context descriptor is seen in many object recognizing applications [10]. The descriptor is however vulnerable to outliers, noise and occlusions and thus is supported by other features as discussed herein.

Edge Orientation is introduced as a similarity feature to ensure robustness against outliers. Literature work presented by [12] illustrate the effective use of edge orientation information to group points that belong to a certain region of interest. This same idea was applied in this situation to ensure point correspondence is only performed between points with similar gradient orientations. The edge orientation cost function (C_{edge}) is calculated as (2), where θ_m and θ_t denote model and target edge orientations. The measure is subsequently normalized to be bounded in [0, 1].

$$C_{edge}(p_m, p_t) = \sum_{n=1}^{N}\left\|\theta_m - \theta_t\right\| \tag{2}$$

The curvature feature information is utilized to ensure further robustness against outliers. The curvature of edge points are calculated using (3), where P_{i-1} and P_{i+1} represent the neighboring points to P_i on shape i.

$$C(p_i) = \left\|p_{i-1} - 2p_i + p_{i+1}\right\| \tag{3}$$

The curvature value in (3) is subsequently bounded in [-1, 1]. Since the curvature is used to compare structurally different objects, normalization is used to stretch the dynamic range onto the entire [-1, 1] interval. This normalization facilitates matching of structurally different regions by assigning curvature values according to rank order, rather than using absolute curvature and thus is scale invariant. The curvature cost function (C_{curv}) is calculated as (4), where $\hat{C}_m$ and $\hat{C}_t$, are the normalized curvature values of the model and target point sets. C_{curv} is intrinsically bounded in [0, 1].

$$C_{curv}(p_m, p_t) = \sum_{n=2}^{N-1}\left\|\hat{C}_m - \hat{C}_t\right\| \tag{4}$$

The Euclidean distance feature information is utilized to ensure continuity of the matched points. The assumption here is that neighboring points on the model should map onto target points which are also close to each other. The importance of figural continuity has been shown by [11]. The Euclidean distance based measure employed can be denoted as (5). The distance term has to be normalized through the external reference term d_0.

$$C_{dist}(p_m, p_t) = \frac{1}{d_0}\sum_{n=1}^{N}\left\|p_m - p_t\right\| \qquad d_0 = \max\left(\left\|p_m - p_t\right\|\right) \tag{5}$$

The overall similarity measure is a weighted combination of the individual similarity measures which are all normalized and bounded between [0, 1]. The total cost of matching the point sets can be minimized through a Bi-partite graph searching methodology. The minimization of the total cost matrix between point sets, P_m and P_t, is subject to the constraint that the matching be one-to-one. This square assignment problem is solved through the Hungarian algorithm with a time complexity of $O(N^3)$.

The correspondences identified through the Hungarian algorithm are then filtered to remove any outliers (incorrectly identified correspondences). This is followed by a regularized thin plate spline (TPS) smoothing to smooth and interpolated the outer contour translations identified (through the non-rigid registration) to the entire projective view (Fig. 3 (a)). Following this the 3D translational field to deform the generic model is created by performing a TPS (un-regularized) interpolation on the sparse translational data identified (Fig. 3 (b)/(c)).

The algorithm iteratively refines and deforms the 3D generic model by continuously performing correspondence estimations, creating the 2D planar translational field (anterior and lateral) and deforming the 3D generic model (Fig. 1).

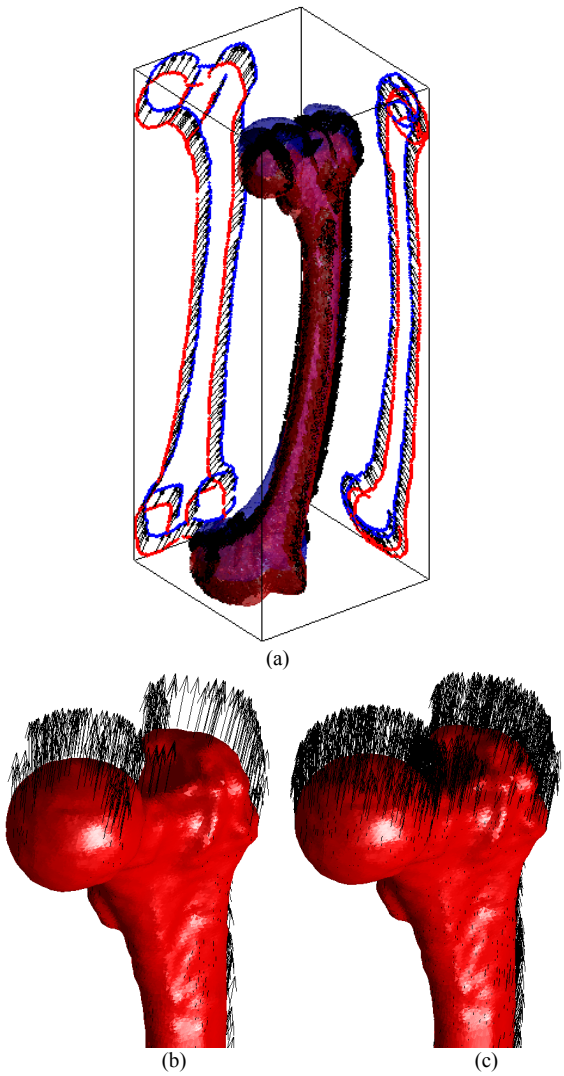

(a) (b) (c)

Figure 3. Non-rigid registration performed on the edge contours and the 3D translational field. From left to right: (a) Non-rigid registration on the sub-sampled edge contour data points for the anterior/lateral views and the associated translational field displayed on the generic model; (b) Close-up of the translations field identified from the planar views displayed on the generic model; (c) TPS based interpolation of the transformation field to deform the generic model.

III. RESULTS

To validate the reconstruction framework, six CT scanned cadaveric femurs (three pairs) and the associated x-ray images in the anterior and lateral view points were utilized in a series of tests. The x-ray images were used for the reconstruction and the corresponding CT scan data for accuracy assessment. Table I shows the quantitative results obtained from the six tests performed. The qualitative result obtained from the one of the six tests performed is shown in Fig. 4(a). The key accuracy measurement used during the testing is the Euclidean distance between the closest points of the reconstructed data and the ground truth CT scan data set. The maximum positive individual Euclidean error identified was 1.26mm and the maximum negative individual error identified was -1.16mm. These results are within the accuracy requirements set by the authors and several other customization studies [6, 9, 13].

TABLE I. INTACT MODEL RECONSTRUCTION TESTING RESULTS

Models Compared	Average Absolute Error (mm)	Standard Deviation (mm)
Right 1/ Right 2	0.82	0.085
Right 1/ Right 3	0.71	0.056
Right 2/ Right 3	0.99	0.091
Left 1/ Left 2	1.05	0.068
Left 1/ Left 3	0.68	0.096
Left 2/ Left 3	0.88	0.078

Furthermore, to test the reconstruction framework's adaptability to other areas of orthopedics, several other individual shape reconstruction tests were performed. These tests involved the tibia and the iliac (pelvic girdle) and have practical relevance due to the potential use of 3D visualization in osteotomy and in hip arthroplasty, as previously mentioned (Fig. 4 (b)/(c)).

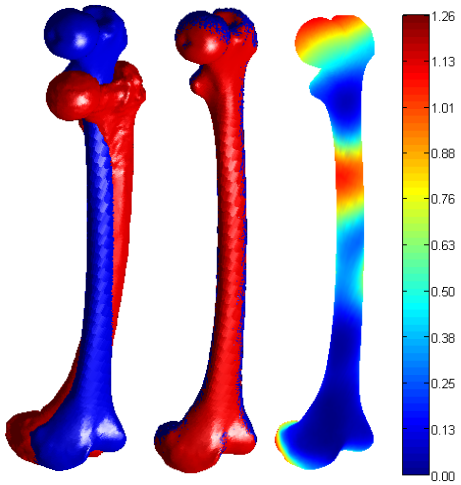

(a)

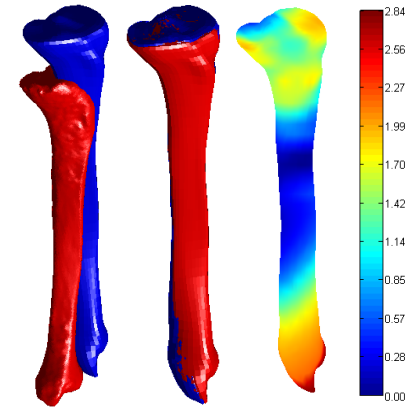

(b)

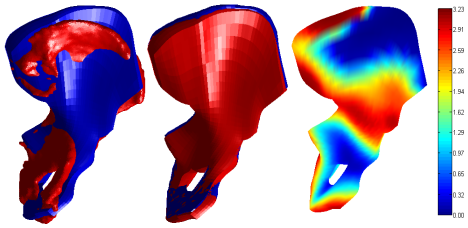

(c)

Figure 4. Several examples of the reconstruction framework being applied. The blue model represents the target model (patient-specific model) while the red model was customized to fit that target utilizing only the anterior and lateral projections. The color bar indicates the absolute error in mm. From left to right: (a) Femur reconstruction; (b) Tibia reconstruction; (c) Iliac reconstruction.

IV. Discussions and Conclusions

This paper demonstrated that using a bi-planar shape customization framework combined with several image processing methodologies can yield acceptable results for patient-specific femur reconstruction. The main criteria required when developing a visualization (reconstruction) methodology for pre-operative planning is the accuracy of reconstruction, adaptability to multiple orthopedic cases and the level of manual intervention required. Time taken is not of a main concern during this pre-operative customization phase. The aforementioned results have indicated that the proposed method has a high accuracy of reconstruction and is adaptable to a multitude of bony anatomies.

A novel registration framework that not only involves the outer contours of the bony anatomy in the reconstruction but also several key interior edges was proposed to enhance customization accuracies and to ensure adaptability to other bony anatomies. The method is based on an iterative non-rigid 2D point matching process and thin-plate spline based deformation. The developed non-rigid registration is robust against disturbances (noise), deformation, outliers and occlusions in the radiographic images.

We have validated the proposed reconstruction framework, through a series of tests conducted with the aid of CT scan data. The accuracy of the reconstruction was adequate for orthopedic surgical planning purposes, which is the target application of the proposed approach.

The proposed bi-planar method has the potential to be used in shape customization of even more difficult bones and to be used in other applications (arthroplasties, osteotomy, etc). Previews of such applications were shown briefly in the Results section. However, as previously mentioned the work presented here is used as a precursor to create 3D fractured bone models to be used intra-operatively by a robotic fracture reduction device. Thus there are several further stages subsequent to the shape customization described here that will incorporate a fracture into the customized bone and will perform a 3D pose-estimation intra-operatively. The integration of this whole system will provide enhanced 3D image guidance to current orthopedic procedures that rely on 2D fluoroscopic images for intra-operative assistance.

References

[1] D. LaRose, L. Cassenti, B. Jaramaz, J. Moody, T. Kanade, and A. DiGioia, "Postoperative measurements of acetabular Cup Position Using X-Ray/CT registration," in *MICCAI*, 2000, pp. 1104-1113.

[2] T. Hüfner, R. Meller, D. Kendoff, J. Zeichen, B. A. Zelle, F. H. Fu, and C. Krettek, "The role of navigation in knee surgery and evaluation of three-dimensional knee kinematics," *Oper. Tech. Orthop.,* vol. 15, pp. 64–69, 2005.

[3] M. Gunay, "Three-dimensional bone geometry reconstruction from X-ray images using hierarchical Free-Form Deformation and non-linear optimization." vol. PhD dissertation Pittsburgh: Carnegie Mellon University, 2003.

[4] J. W. Fernandez, P. Mithraratne, S. F. Thrupp, M. H. Tawhai, and P. J. Hunter, "Anatomically based geometric modelling of the musculo-skeletal system and other organs," *Biomech. Model Mechanobiol,* vol. 2, pp. 139–155, 2004.

[5] L. Caponetti and A. M. Fanelli, "Computer-aided simulation for bone surgery," *IEEE Comput. Graph. Appl.,* vol. 13, pp. 86–92, 1993.

[6] G. Zheng and L.-P. Nolte, "Surface Reconstruction of Bone from X-ray Images and Point Distribution Model Incorporating a Novel Method for 2D-3D Correspondence," in *Proceedings of the IEEE Computer Society Conference on Computer Vision and Pattern Recognition*, 2006.

[7] M. Fleute and S. Lavallée, "Building a complete surface model from sparse data using statistical shape models: application to computer assisted knee surgery system," in *MICCAI*, Heidelberg, 1998, pp. 879–887.

[8] S. Benameur, M. Mignotte, and S. Parent, "A hierarchical statistical modeling approach for the unsupervised 3D biplanar reconstruction of the scoliotic spine," *IEEE Trans. Biomed. Eng,* vol. 52, pp. 2041–2057, 2005.

[9] B. Schmutz, K. J. Reynolds, and J. P. Slavotinek, "Customization of a generic 3D model of the distal femur using diagnostic radiographs," *Journal of Medical Engineering & Technology,* vol. 32, pp. 156 – 161, 2008.

[10] S. Belongie, J. Malik, and J. Puzicha, "Shape Matching and Object Recognition Using Shape Contexts," *IEEE Transactions on Pattern Analysis and Machine Intelligence,* vol. 24, pp. 509-522, 2002.

[11] A. Thayananthan, B. Stenger, P. H. S. Torr, and R. Cipolla, "Shape context and chamfer matching in cluttered scenes," in *Proceedings of the IEEE Computer Society Conference on Computer Vision and Pattern Recognition*, 2003, pp. I/127-I/133.

[12] C. F. Olson and D. P. Huttenlocher, "Automatic target recognition by matching oriented edge pixels," *Transactions on Image Processing,* vol. 6, pp. 103–113, January 1997.

[13] P. Gamage, S. Q. Xie, P. Delmas, P. Xu, and S. Mukherjee, "Radiograph Based Patient-Specific Customization of a Generic Femur," in *Mechatronics and Machine Vision in Practice, 2008. M2VIP 2008. 15th International Conference on*, 2008, pp. 622-627.